Estuarine, Coastal and Shelf Science
October 2019, Volume 226 Pages 106263 (9p.)
https://doi.org/10.1016/j.ecss.2019.106263
https://archimer.ifremer.fr/doc/00505/61617/

Mangroves and shoreline erosion in the Mekong River delta, Viet Nam

Besset Manon [1, 2, *] , Gratiot Nicolas [3, 4], Anthony Edward J. [1, 5], Bouchette Frédéric [1], Goichot Marc [6], Marchesiello Patrick [7]

[1] University of Montpellier, Geoscience Montpellier, Montpellier, France
[2] Aix Marseille University, CNRS, IRD, INRA, Coll France, CEREGE, Aix-en-Provence, France
[3] CARE, Ho Chi Minh City University of Technology, VNU-HCM, Viet Nam
[4] Université Grenoble Alpes, CNRS, IRD, Grenoble INP, IGE, F-38000, Grenoble, France
[5] USR LEEISA, CNRS, Cayenne, French Guiana
[6] Lead, Water, WWF Greater Mekong Programme, 14B Ky Dong Street, Ward 9, District 3, Ho Chi Minh, Viet Nam
[7] IRD, LEGOS, 14 Avenue Edouard Belin, 31400, Toulouse, France

* Corresponding author : Manon Besset, email address : manon.besset@gm.univ-montp2.fr

Abstract :

The question of the rampant erosion of the shorelines rimming the Mekong River delta has assumed increasing importance over the last few years. Among issues pertinent to this question is how it is related to mangroves. Using high-resolution satellite images, we compared the width of the mangrove belt fringing the shoreline in 2012 to shoreline change (advance, retreat) between 2003 and 2012 for 3687 cross-shore transects, spaced 100 m apart, and thus covering nearly 370 km of delta shoreline bearing mangroves. The results show no significant relationships. We infer from this that, once erosion sets in following sustained deficient mud supply to the coast, the rate of shoreline change is independent of the width of the mangrove belt. Numerous studies have shown that: (1) mangroves promote coastal accretion where fine-grained sediment supply is adequate, (2) a large and healthy belt of fringing mangroves can efficiently protect a shoreline by inducing more efficient dissipation of wave energy than a narrower fringe, and (3) mangrove removal contributes to the aggravation of ongoing shoreline erosion. We fully concur, but draw attention to the fact that mangroves cannot accomplish their land-building and coastal protection roles under conditions of a failing sediment supply and prevailing erosion. Ignoring these overarching conditions implies that high expectations from mangroves in protecting and/or stabilizing the Mekong delta shoreline, and eroding shorelines elsewhere, will meet with disappointment. Among these false expectations are: (1) a large and healthy mangrove fringe is sufficient to stabilize the (eroding) shoreline, (2) a reduction in the width of a large mangrove fringe to the benefit of other activities, such as shrimp-farming, is not deleterious to the shoreline position, and (3) the effects of human-induced reductions in sediment supply to the coast can be offset by a large belt of fringing mangroves.

Highlights

► We compared Mekong delta shoreline change between 2003 and 2012 and width of fringing mangroves. ► We found no significant relationships between the rate of shoreline change and mangrove width. ► Large tracts of the delta shoreline are eroding due to inadequate mud supply. ► When mud supply replenishment is low, even a wide mangrove belt will retreat. ► Mangrove protection initiatives need to consider sustained sediment supply as a key parameter.

Keywords : Mangroves, Mekong river delta, Shoreline erosion, Coastal squeeze, Sediment supply

1. Introduction

Mangroves are halophytic (tolerant to saline waters) coastal forests that develop at the interface between muddy shores and mostly brackish waters. Mangroves are characteristic of many tropical and subtropical coastlines between 32°N and 38°S (Brander et al., 2012). An ecosystem in its own right, mangroves shelter various fauna, and the thriving and survival of which are totally dependent on healthy mangroves. A wide and healthy belt of mangroves fringing the shoreline also plays a significant role in contributing to coastal protection by dissipating waves under normal energetic ocean forcing conditions. This protective role has been demonstrated in several studies conducted theoretically (Massel et al., 1999), in the laboratory (Hashim and Catherine, 2013), and from field monitoring (Mazda et al., 1997; Quartel et al., 2007; Barbier et al., 2008; Horstman et al., 2014), but also from geomorphological and coastal management-oriented approaches (Anthony and Gratiot, 2012; Winterwerp et al., 2013; Phan et al., 2015). The protective role of mangroves during the course of extreme climatic and tsunami events and disasters has been underlined (e.g., Alongi, 2008; Gedan et al., 2011; Marois and Mitsch, 2015). Mangroves are closely linked with their physical environment and contribute to land-building by trapping sediment through their complex aerial root structure (e.g., Carlton, 1974; Kathiresan, 2003; Anthony, 2004; Corenblit et al., 2007; Kumara et al., 2010). By contributing to delta aggradation, mangroves mitigate sea-level rise effects induced by climate change, which in turn are a threat to this ecosystem (Gilman et al., 2007; McKee et al., 2007; Gedan et al., 2011; Woodroffe et al., 2016). Healthy mangroves can trap more than 80% of incoming fine-grained sediment (Furukawa et al., 1997) and contribute to sedimentation rates of the order of 1-8 mm/year, generally higher than local rates of mean sea-level rise (Gilman et al., 2006; Gupta, 2009; Horstman et al., 2014).

On coasts characterized by mangroves, resilience to high-energy events such as tsunami or repeated storms can be impaired where mangrove loss has been generated and sustained by human activities. This can be envisaged through consideration of the concept of the tipping point, which corresponds to a threshold value beyond which a system cannot return to its original dynamic equilibrium (Kéfi et al., 2016). Tipping points occur where one or more of the driving processes go beyond a threshold, resulting in destabilized dynamic feedback loops that link all processes together. This can be expected where the sediment supply is drastically reduced (sediment trapping by dams, sand mining, etc.), or where oceanic forcing is modified over a long period of time (18.6-year tidal cycles, ocean oscillations, etc.). This is also the case where a mangrove fringe is reduced in width by coastal ‘squeeze’ or by deforestation (Lewis, 2005; Anthony and Gratiot, 2012). Coastal squeeze occurs where anthropogenic modifications on the coast lead to a significant cross-shore reduction of coastal space (Doody, 2004; Pontee, 2013; Torio and Chmura, 2013). A number of case studies have shown that coastal squeeze can lead to coastal erosion, including in areas where mangroves occur (e.g., Heatherington and Bishop, 2012; Anthony and Gratiot, 2012; Winterwerp et al., 2013; van Wesenbeeck et al., 2015; Toorman et al., 2018; Brunier et al., 2019). van Wesenbeeck et al. (2015) have highlighted mangrove sensitivity to human pressures and the feedback effects resulting from conversion of mangrove lands to intensive aquaculture that generates coastal erosion. This leads to a breakdown of the buffer effect of the mangrove forest on wave energy and in promoting sediment trapping. This alteration can encourage accelerated erosion (Mitra, 2013). In addition, in the case of aquaculture and agriculture, the river channels commonly become disconnected from the natural floodplain to the benefit of farming, which results in a significant reduction of sediment supply to the floodplain. A particularly overlooked area in gauging the significance of mangroves is that of adequate sediment supply, an overarching background factor without which the commonly considered 'land-building' role of mangroves cannot be successful. Mangroves are limited producers of sediment (organic or authigenic production), whereas the negative effects of the reduction of allogenic sediment supply by rivers caused by trapping by dam reservoirs and by sand mining are often aggravated by accelerated subsidence and sea-level rise. Both create accommodation space that then requires more sediment to maintain mangrove substrate elevations.

The Mekong delta in Viet Nam (Fig. 1), the third largest delta in the world (Coleman and Huh, 2004), has a particularly well-developed mangrove environment (Veettil et al., 2019). The delta makes up for 12 % of the country's natural land and 19 % of its national population, and hosts a population of 20 million inhabitants (Mekong River Commission, 2010). The delta is crucial to the food security of Southeast Asia, and provides 50% of Viet Nam's food (General Statistics Office of Viet Nam) and is part of a river with the most concentrated fish biodiversity per unit area of any large river basin in the world, with 454 fish species in the delta alone (Vidthayanon, 2008), and ranking second only to the Amazon in overall biodiversity (WWF, 2012). As the country's largest agricultural production centre, the delta region contributes half of Viet Nam's rice output, 65 percent of aquatic products and 70 percent of fruits. It also accounts for 95 percent of the country's rice exports and 60 percent of total overseas shipment of fish. Following the ravages of the Viet Nam War (1960-1972) on the delta's forests, these important advantages have significantly impacted the mangroves of the delta, notably in the muddy southwestern and Gulf of Thailand areas where large tracts have been removed to provide timber for charcoal and for the construction industry, and to make place for shrimp farms and aquaculture (Phan and Hoang, 1993; Christensen et al., 2008; Veettil et al., 2019). Several recent studies have also shown that erosion is becoming increasingly rampant along much of the delta shoreline (Anthony et al., 2015; Besset et al., 2016; Allison et al., 2017; Li et al., 2017), leading to the recurrent displacement of coastal populations (Boateng, 2012) and increasing recourse to coastal protection structures, notably dykes (Albers and Schmitt, 2015). Sea dykes are being increasingly built along parts of the muddy East Sea and Gulf of Thailand coasts for protection from marine flooding and for shrimp farms, generating a process of 'mangrove squeeze' (Phan et al., 2015).

The erosion of the Mekong delta has been attributed to sediment depletion associated with three main factors (Anthony et al., 2015): (1) potential trapping of sediment by the increasing number of dams constructed in the Mekong catchment, (2) large-scale commercial sand mining in the river and delta channels, and (3) accelerated subsidence due to groundwater pumping. With regards to the first two factors, recent studies have documented a marked reduction in the sediment load of the Mekong River reaching the delta from 160 Mt/yr in 1990 to 75 Mt/yr in 2014 (Koehnken, 2014), and maybe even down to 40 ±20 Mt/yr currently (Piman and Shrestha, 2017; Ha et al., 2018). This reduction also generates mechanisms of sediment redistribution by waves and currents that could explain exacerbated shoreline erosion in places (Marchesiello et al., 2019). 38% of the Mekong delta region is at risk of being underwater by the year 2100 (https://en.vietnamplus.vn/forum-to-talk-climateresilient-development-in-mekong-delta/145888.vnp), with a large contribution to this from subsidence generated by massive groundwater extraction (Minderhoud et al., 2017). Anthony et al. (2015) also suggested, however, that marked alongshore variability in erosion rates may also be influenced by differences arising from the presence and protective role of mangroves, or their absence which may enhance erosion. Mangrove loss thus comes out as an additional factor in modulating erosion of the Mekong delta. Phan et al. (2015) showed that dissipation of waves incident on the delta shoreline was not effective where mangroves had been removed, especially in the case of infragravity waves which require a large mangrove cover several hundred metres wide to be significantly attenuated, such that mangrove removal indeed contributed to shoreline erosion. On the basis of 18 individual cross-shore profiles distributed along about 320 km of deltaic coast from the mouths of the Mekong to Ca Mau Point (Fig. 1), Phan et al. (2015) showed a net correlation between mangrove width and local erosion or accretion. Notwithstanding their limited number of data points and the large error bars of these points, Phan et al. (2015) identified a minimum critical width of 140 m for a stable mangrove fringe, and, above this minimum width, a capacity to promote sedimentation. The authors considered that the larger the width of the mangrove fringe the more efficient the attenuation of waves and currents will be, offering a successful environment for both seedling establishment and sedimentation. Indeed, this relationship is in agreement with numerous previous studies showing that the larger the mangrove width, the better the protection offered by mangroves against waves (e.g., Barbier et al., 2008). However, this finding is pertinent to wave energy being dissipated across a more or less broad mangrove belt, which is not quite the same thing as mangrove protection against an ongoing erosion process. Furthermore, an environment for successful mangrove seedling requires that substrate accretion levels are maintained by sustained sediment supply (Balke et al., 2011).

The objective of this paper is to further test the relationship described by Phan et al. (2015) based on the rationale that the shoreline change trends deduced from satellite images in recent studies may be correlated with mangrove width identified on the same satellite images. We first compare mangrove width and shoreline change over cross-shore profiles at the scale of the entire delta, then at the scale of the three deltaic sectors commonly identified along the Mekong delta (e.g., Anthony et al., 2015): the delta distributary mouths sector (0-280 km), the 'East Coast' (280-379 km) bordering the South Sea, and the 'West Coast' in the Gulf of Thailand (379-564 km) (Fig. 1). Following this, we gauged the relationship between mangroves and shoreline change in the delta.

2. Data and Methods

2.1 Remote-sensing data

Using a relevant cartographic frame (Projection UTM 48N), a baseline *B* was set about 1 km offshore (Fig. 2) of the Mekong delta shoreline. This baseline was regular enough to: (i) smooth any small-scale instabilities related to a non-rectilinear shoreline, and (ii) delineate large-scale geomorphic features such as capes or bays. We then set up regularly spaced transects perpendicular to the baseline and extending from offshore to 3 kilometres inland. Following this, we projected a set of 43 high-resolution SPOT 5 level 3 ortho-rectified colour satellite images for January 2003 (2003) and December 2011/February 2012 (2012) at a scale of 1:10,000 within the cartographic frame. These images, initially described in Anthony et al. (2015), cover the ≈ 500 km of delta shoreline. The SPOT 5 images are 5 m pixel-resolution panchromatic images (spectral band within 0.48-0.71 µm) acquired in pairs simultaneously with a half-pixel spatial shift. The resulting SPOT 5 Super-Mode images offer a final resolution of 2.5 m appropriate for precisely locating the shorelines and the edges of the mangrove fringe. This is the best theoretical spatial resolution for the study.

2.2. Extraction of shorelines and mangrove limits

There is no standardized definition of the shoreline (e.g., Boak and Turner, 2005; Ruggiero and List, 2009) and this implies the choice of a yardstick, preferably one that can be re-used in successive surveys, to identify a position of the land-water interface. Following extensive field observations covering over 300 km of the Mekong delta's shoreline over the period 2011-2012, Anthony et al. (2015) suggested the use of the seaward limit of vegetation as the shoreline. The brush/plantation fringe in sectors of sandy coast characterized by beaches, and the mangrove fringe in the muddy sectors, were adopted as good 'shoreline' markers. We used the shoreline digitized in Anthony et al. (2015) from the 2003 and 2012 images using the automatic digital shoreline analysis DSAS (Himmelstoss et al., 2018), and traced 4155 new cross-shore transects, spaced 100 m alongshore. This alongshore spacing appeared to provide the best compromise between precision and the overall length of analyzed delta shoreline (415 km). Phan et al. (2015) selected a set of only 18 transects to define the relationship between mangrove width and shoreline change over the period 1989-2002. Our study is based on the systematic analysis of a much larger set of transects but also concerns a more recent period marked by increasing erosion of the delta (Anthony et al., 2015; Li et al., 2017). Transects through mangrove vegetation were retained as the primary basis for our analysis. It may be noted that at least half of the transects used by Phan et al. (2015) could not have concerned mangrove-bearing shorelines since they went through sandy (open beach-foredune) portions of the river-mouth sector (see their Fig. 1B). 45% (113 km out of 250 km) of the delta's shoreline is characterized by 'upland' brush-plantation vegetation associated with these beaches and foredunes in the river-mouth sector (Anthony et al., 2015). We digitized the inland limit of the mangrove fringe using the same procedure as Phan et al. (2015). This consisted in using dikes observed on satellite images as this inland limit (Fig. 2).

Along each cross-shore transect superimposed on these images, we digitised the following curves:

- S_{2003}: the shoreline in 2003,
- S_{2012}: the shoreline in 2012,
- M_{inland}: the line defining the 2012 inland limit of vegetation up to the main dike,
- M_{shore}: the line defining the 2012 seaward limit of vegetation.

Since the issue at hand here is simply that of determining the relationship between the width of a mangrove fringe at a time *t* with shoreline change over several years, we had a choice between the 2003 and 2012 satellite images. The results yielded by the two datasets are virtually identical (Supplementary Material 1). We preferred, thus, the 2012 images which are are of better quality than those of 2003, especially for delimiting the landward vegetation fringe, and the comparison is coherent with that adopted by Phan et al. (2015).

We extracted the positions of the four digitized lines at the intersection with each cross-shore profile. Thus, in the cartographic frame, we obtained four sets of shorelines and limits of mangroves: $(X_{2003}^i; Y_{2003}^i)_{i\in[1:N]}$, $(X_{2012}^i; Y_{2012}^i)_{i\in[1:N]}$, $(X_{inland}^i; Y_{inland}^i)_{i\in[1:N]}$, and $(X_{shore}^i; Y_{shore}^i)_{i\in[1:N]}$ where *i* refers to a cross-shore profile and *N* is the total number of cross-shore profiles. In addition, we obtained the set $(X_B^i; Y_B^i)_{i\in[1:N]}$ of node coordinates along the baseline from which each cross-shore transect commences.

Using these five datasets, we determined the following distances to the baseline:

- the distance of the 2003 shoreline

$$S_{2003}^i = \sqrt{(X_{2003}^i - X_B^i)^2 + (Y_{2003}^i - Y_B^i)^2} \quad (1)$$

- the distance of the 2012 shoreline

$$S_{2012}^i = \sqrt{(X_{2012}^i - X_B^i)^2 + (Y_{2012}^i - Y_B^i)^2} \quad (2)$$

- the distance of the 2012 inland edge of the mangrove fringe

$$M_{inland}^i = \sqrt{(X_{inland}^i - X_B^i)^2 + (Y_{inland}^i - Y_B^i)^2} \quad (3)$$

- the distance of the 2012 seaward edge of the mangrove fringe

$$M^i_{shore} = \sqrt{(X^i_{shore} - X^i_B)^2 + (Y^i_{shore} - Y^i_B)^2} \quad (4)$$

We calculated the mean annual rate of shoreline change V^i_S at each cross shore transect i:

$$V^i_S = \frac{S^i_{2003} - S^i_{2012}}{\Delta T} \quad (5)$$

where ΔT is the time interval between the two consecutive SPOT 5 surveys (9 years). We also calculated the current width of the mangrove fringe W^i at each cross-shore transect i:

$$W^i = M^i_{inland} - M^i_{shore} \quad (6)$$

Following these procedures, we carried out analysis of possible relationships between V^i_S and W^i at various spatial scales, by considering various subsets of cross-shore transects. A few stretches of shoreline (less than 5% overall) could not be analyzed because of various technical problems such as cloud cover, thin (< 10 m wide) residual mangrove fringe, or where the edge of mangroves was not readily distinguishable on the images. Finally, taking into account these limitations, we obtained 3687 relevant pairs of shoreline change (V^i) and mangrove width (W^i).

2.3. Error margins and uncertainty

Anthony et al. (2015) demonstrated that a good estimate of E_V, the mean uncertainty for V^i, is of the order of ±5 m/yr for all of the cross-shore transects. In this paper, we needed to define the margin of error in the quantification of W^i. To do so, we considered E_P [m], the total error in the positioning of the points defining mangroves inland and the limits of the shore (Fletcher et al., 2003; Rooney et al., 2003; Hapke et al., 2006):

$$E_P = E_r^2 + E_g^2 + E_c^2 \quad (7)$$

The three mean squared errors are relative to: (i) E_r [m] the image resolution, (ii) E_g [m] the SPOT 5 georeferencing, and (iii) E_c [m] the size of the cursor used to digitize the mangrove fringe line (which depends on the scale at which the image is plotted during digitizing). Fletcher et al. (2003), Rooney et al. (2003), and Hapke et al. (2006) considered tidal fluctuations as a possible alternative source of uncertainty in E_P. To handle this problem, we checked that the SPOT 5 images in 2012 were shot more or less at the same moment in the tidal cycle. Thus, this contribution remains very negligible and was not considered further in this study.

Practically, E_c was set to 2.8 m precisely for the study. E_g varied from 1.4 to 2.9 m. E_r was 2.5 m as explained above. As a consequence, we had a mean positioning uncertainty E_P ranging from 4.0 to 4.7 m. We considered this margin of error as constant throughout for all the 3687 profiles. Finally, we calculated E_W[m] the mean uncertainty for the mangrove fringe widths W^i for all the transects as being the quadratic error of positioning at the inland and seaward limits of the mangrove fringe:

$$E_W = \frac{1}{N}\sum\left(\sqrt{E_{inland}^2 + E_{shore}^2}\right) \quad (8)$$

where E_{inland} is the positioning error defined for the inland limit of the mangrove width and E_{shore} that of the seaward limit. As the SPOT 5 images are the same for seaward and inland limit digitizing, $E_{inland} = E_{shore}$, which meant that:

$$E_W = \frac{\sqrt{2}}{N}\sum_1^N E_P \quad (9)$$

3. Results

The statistical comparison between shoreline change and coastal mangrove width is carried out at two scales: regional and local.

3.1 Regional scale (river-mouths/East Coast/West Coast)

When all 3687 transects are considered, there are no statistical correlations at the larger, regional scale (Fig. 4). 31% (≈80 km) of eroded shorelines are bordered by a mangrove width larger than the upper limit of a 500 m-wide mangrove fringe proposed by Phan et al. (2015) to ensure sediment trapping. Delimiting a threshold is difficult when all the data are taken into account without sorting. We therefore resorted to discretization and ranking of the results.

The results obtained thus show a decline in the number of cross-shore eroding transects as the width of the mangrove fringe increases (Fig. 4). In the delta distributary mouths, a decrease in the proportion of eroding transects in favour of that of prograding transects is observed, with mangrove width increasing until a threshold of 400 m. In this sector, only 8.5% (116 out of the 1370 profiles) of the shoreline shows a direct linear relationship between mangrove width and the rate of erosion/accretion.

Along the East and West Coasts, no trend comes out, the percentage of transects in erosion varying only slightly as a function of mangrove width (Fig. 4B). In fact, the number of erosional transects along the East Coast increases despite large mangrove widths, whereas the number of those in the mouths sector and the West Coast decrease (i.e. 0.6–1.2 km-wide mangrove). The results also show that the East Coast is largely dominated by erosion (97% of black dots in Fig. 3), even though the width of the mangrove belt exceeds 2 km in places.

3.2 Local scale (5 km-long transects)

To go further into the analysis, we divided the shoreline into longshore segments of 5 km (50 consecutive transects) (Fig. 5). At this scale, we integrated transects with non-mangrove vegetation at the delta distributary mouths. Each line in the figure represents a coastal segment where a linear trend is observed. Along the 482 km of shoreline analyzed (including 113 km of shoreline with 'upland' brush-plantation vegetation), we identified only nine segments of deltaic shoreline, exclusively in the mouths sector and the West Coast, showing a significant relationship $r^2 > 0.75$, up to 1) between mangrove width and shoreline change (Fig. 5). Each segment has an alongshore length ranging from 0.5 to 5 km (5 to 50 consecutive points separated 100 m alongshore are aligned in Fig. 3). These segments represent a cumulative length of 37 km, i.e. ≈10% of the total length of analyzed shoreline. Of this, 16.6 km correspond to shoreline segments with non-mangrove vegetation.

4. Discussion

At the overall regional scale, our results reveal a pattern that is more complex than the simple linear relationship proposed by Phan et al. (2015) between mangrove width and the status of the shoreline in the Mekong delta. The results obtained in the present study, and based on a comprehensive analysis of 3687 pairs of shoreline change and mangrove width spaced 100 m (i.e., covering a total shoreline length of 369 out of ca. 500 km of delta shoreline), show no statistically significant relationships, whatever the scale considered (Figs. 3, 4, 5). This goes with the field observations of Anthony et al. (2015) who reported active and quasi-continuous alongshore erosion of muddy mangrove-bearing bluffs along much of the East and West Coasts in 2012. Two immediate inferences that come out of these findings are: (1) that a large mangrove width is not necessarily tantamount to shoreline progradation in the Mekong delta; (2) the overarching role of prevailing erosion which, where established, leads to sustained shoreline retreat, whatever the width of the mangrove belt. There is no doubt that mangroves, by dissipating waves and currents, can contribute actively to protection of a variably wide coastal fringe (which is not quite the same thing as protection of the shoreline on which waves impinge), and can, especially, promote rapid coastal accretion where fine-grained sediment supply is adequate, or delay, but not halt, coastal retreat, where the sediment supply is inadequate. Our study shows, however, that for ≈90% of the Mekong delta shoreline, the relationship between mangroves and how the shoreline evolves needs to be carefully considered in a context that takes into account antecedent and prevailing shoreline erosion or accretion. These situations of erosion or accretion are, in turn, vested in the larger-scale control exerted by alongshore adjustments between net sediment supply or availability, wave and current energy, and sediment redistribution by waves and currents (Anthony et al., 2015; Marchesiello et al., 2019). Ignoring these basic aspects may imply that high expectations from mangroves could be met with disappointment. This can have important shoreline management implications because of the following wrong deductions: (1) a large mangrove fringe is enough to stabilize a (eroding) shoreline, (2) some reduction of the mangrove width to the benefit of other activities such as shrimp-farming is not deleterious, and (3) the effects of human-induced reductions in sediment supply to the coast can be offset by mangroves.

The foregoing points simply warn that the efficiency of mangroves in assuring shoreline stability needs to be viewed in the light of the established (decadal) shoreline trend, which, in turn, is determined by sediment supply and hydrodynamic conditions. The protective capacity of mangroves can be particularly impaired where sediment supply is in strong or persistent deficit, fine examples being the mangrove-rich Guianas coast between the Amazon and Orinoco river mouths, the world's longest muddy coast (Anthony and Gratiot, 2012). Here, so-called decadal to multi-decadal 'inter-bank' phases of relative mud scarcity separating mud-rich 'bank' phases (discrete mud banks migrating alongshore from the mouths of the Amazon are separated by inter-bank zones of erosion) can be characterized by rates of shoreline erosion that can exceed 150 m/year notwithstanding the presence of dense mangrove forests up to 30 m high and forming stands several km-wide (Brunier et al., 2019).

The width of the energy-dissipating mangrove fringe alone does not play a determining role, neither in the context of erosive oceanic forcing, nor in the context of decreasing sediment supply to the delta. This reflects a tipping-point effect wherein once sediment supply to the coast is in chronic deficit (a deficit aggravated by delta-plain trapping to compensate for accelerated subsidence), the vertical growth of shorefront mudflats is no longer assured. Mangrove colonization can be precluded where shorefront mudflat elevations are below a tidal level threshold to enable seedling establishment (Proisy et al., 2009; Balke et al., 2011, 2013). Shorefront substrate elevations in the Mekong delta have not been monitored, but these unfavourable conditions for mangroves are likely exacerbated by: (1) narrowing of the mangrove fringe which entails less wave dissipation and therefore decrease in turbulence dissipation and flocculation (Gratiot et al., 2017); and (2) the increasing number of aquaculture farms and dykes to protect rice farms, limiting the tidal prism with negative effects on sediment trapping (Li et al., 2017). At the local scale of a few km, increasing mangrove width can be correlated with shoreline change, as at km $\approx$ 455 in the southern extremity of the delta, near Ca Mau point (Fig. 1), where there appears to be convergence of suspended mud (Marchesiello et al., 2019). Hence, the pertinence of a comparative analysis at different scales (local/individual transects, alongshore segments, delta mass as a whole representing the entire river basin).

Reflections on coastal management and coastal protection measures adapted to the Mekong delta imply acquiring a good grasp of the resilience of the delta's mangroves. Efforts aimed jointly at maintaining and preserving, rather than further destroying, mangroves (Jhaveri and Nguyen, 2018; Veettil et al., 2019), and in assuring sustained sediment supply to the delta shores, will also be required in the years to come.

5. Conclusions

1. The width of the mangrove fringe rimming 369 km (≈ 90%) of the Mekong delta shoreline, and shoreline change between 2003 and 2012, were determined for 3687 cross-shore transects spaced 100 m apart from a comparison of high-resolution satellite images. The results show that 68% of the delta shoreline is undergoing erosion and 91% of the eroding shoreline is characterized by mangroves.

2. Statistical relationships between shoreline change and mangrove width were determined: (a) at the scale of the entire dataset of 3687 transects, (b) at the scale of the three sectors composing the delta shoreline: the delta distributary mouths, dominantly characterized by sandy beach-dune shorelines, and which was therefore largely excluded from this analysis, and the muddy East and West coasts, hitherto rich in mangroves, and, (c) at a more local level comprised of transects over shoreline segments of 5 km.

3. The results show no significant trend, whatever the level considered. This finding differs from that of Phan et al. (2015) who depicted, on the basis of only 18 data points, a linear relationship between reduced mangrove width and coastal erosion. A linear relationship was observed in a very few sectors accounting for less than 5.5% of the entire delta shoreline.

4. Phan et al. (2015) identified a minimum critical width of 140 m for a stable mangrove fringe, and above this width, a capacity for mangroves to promote sedimentation. Although a wide and healthy mangrove fringe is desirable, the 140 m-width recommended by Phan et al. (2015) is not a scientifically defensible width.

5. Our results indicate that the role of mangroves in coastal protection needs to be carefully considered in a context that takes into account antecedent prevailing shoreline erosion or accretion vested in the larger-scale alongshore adjustments between net sediment supply and the ambient coastal dynamics driven by waves and currents.

6. Beyond a certain threshold of deficient mud supply, and under maintained ambient hydrodynamic conditions, mangroves, whatever their width, can no longer assure shoreline advance or even stability, although they contribute to the attenuation of erosion by waves and currents.

7. Although erosion of mangrove-colonized shorelines results from natural morpho-sedimentary adjustments driven by sediment supply and hydrodynamic forcing, mangroves can contribute actively to coastal protection even under a context of shoreline erosion. Mangrove removal contributes, thus, to the aggravation of shoreline erosion.

8. Reflections on coastal protection in the Mekong delta require not only a good knowledge of the resilience of mangroves, efforts aimed at preserving them, but also understanding the large-scale processes (source-to-sink sediment supply, oceanic forcing, climate change) that assure sustained sediment supply to the delta shores, building and maintaining the delta in a dynamic equilibrium.

Acknowledgements

We acknowledge initial joint funding from Fond Français pour l'Environnement Mondial (FFEM) and WWF Greater Mekong. Further support was provided by the ANR-Belmont Forum Project 'BF-Deltas: Catalyzing Action Towards Sustainability of Deltaic Systems with an Integrated Modeling Framework for Risk Assessment', and by the Lower Mekong Delta Coastal Zone project (LMDCZ, EU-AFD & SIWRR, 2018). The SPOT 5 images were provided by the CNES/ISIS programme (© CNES 2012, distribution Spot Image S.A.). We thank Colin Woodroffe and an anonymous reviewer for their insightful comments and suggestions.

References

Albers, T., Schmitt, K., 2015. Dyke design, floodplain restoration and mangrove co-management as parts of an area coastal protection strategy for the mud coasts of the Mekong delta, Vietnam. Wet. Ecol. Manag., 23, 6, 991–1004. https://doi.org/10.1007/s11273-015-9441-3

Allison, M.A., Nittrouer C.A., Ogston, A.S., Mullarney, J.C., Nguyen, T.T, 2017. Sedimentation and survival of the Mekong Delta: A case study of decreased sediment supply and accelerating rates of relative sea level rise. Oceanography 30, 98–109, https://doi.org/10.5670/oceanog.2017.318.

Alongi, D.M., 2008. Mangrove forests: Resilience, protection from tsunamis, and responses to global climate change. Estuar. Coast. Shelf Sci., 76, 1, 1 - 13. https://doi.org/10.1016/j.ecss.2007.08.024

Anthony, E.J., 2004. Sediment dynamics and morphological stability of an estuarine mangrove complex: Sherbro Bay, West Africa. Mar. Geol., 208, 207-224.

Anthony, E.J., Brunier, G., Besset, M., Goichot, M., Dussouillez, P., Nguyen, V.L., 2015. Linking rapid erosion of the Mekong River delta to human activities. Sci. Rep., 5, 1–12. http://dx.doi.org/10.1038/srep14745

Anthony, E.J., Gratiot, N., 2012. Coastal engineering and large-scale mangrove destruction in Guyana, south America: Averting an environmental catastrophe in the making. Ecol. Eng., 47, 268 - 273. https://doi.org/10.1016/j.ecoleng.2012.07.005

Balke, T., Bouma, T.J., Horstman, E.M., Webb, E.L., Erftemeijer, P.L.A., Herman, P.M.J., 2011. Windows of opportunity: thresholds to mangrove seedling establishment on tidal flats. Marine Ecological Progress Series, 440, 1–9.

Balke, T., Webb, E.L., van den Elzen, E., Galli, D., Herman, P.M.J., Bouma, T.J., 2013. Seedling establishment in a dynamic sedimentary environment: a conceptual framework using mangroves. J. Appl. Ecol., 50, 740–747.

Barbier, E.B., Koch, E.W., Silliman, B.R., Hacker, S.D., Wolanski, E., Primavera, E.J., Granek, E.F., Polasky, S., Aswani, S., Cramer, L.A., Stoms, D.M., Kennedy, C.J., Bael, D., Kappel, C.V., Perillo G.M.E., Reed, D. 2008. Coastal ecosystem based management with non-linear ecological functions and values. Science, 319, 321.

Besset, M., Anthony, E.J., Brunier, G., Dussouillez, P., 2016. Shoreline change of the Mekong River delta along the southern part of the South China Sea coast using satellite image analysis (1973-2014). Géomorphologie, 22, 2, 137-146. http://dx.doi.org/10.4000/geomorphologie.11336

Boak, E.H., Turner, I.L., 2005. Shoreline definition and detection: A review. Journal of Coastal Research, 21, 688-703.

Boateng, I., 2012. GIS assessment of coastal vulnerability to climate change and coastal adaption planning in Vietnam. J. Coast. Conserv., 16, 1, 25–36. https://doi.org/10.1007/s11852-011-0165-0

Brander, L.M., Wagtendonk, A.J., Hussain, S.S., McVittie, A., Verburg, P.H., Groot, R.S., Ploeg, S., 2012. Ecosystem service values for mangroves in Southeast Asia: a meta-analysis and value transfer application. Ecosyst. Serv., 1, 62–69. https://doi.org/10. 1016/j.ecoser.2012.06.003.

Brunier, G., Anthony, E.J., Gratiot, N., Gardel, A., 2019. Exceptional rates and mechanisms of muddy shoreline retreat following mangrove removal. Earth Surf. Process. Landf., 44, 1559-1571. https://doi.org/10.1002/esp.4593.

Carlton, J.M., 1974. Land-building and stabilization by mangroves. Environ. Conserv., 1, 4, 285294. https://doi.org/10.1017/S0376892900004926

Christensen, S.M., Tarp, P., Hjortso, C.N., 2008. Mangrove forest management planning in coastal buffer and conservation zones, Vietnam: A multimethodological approach incorporating multiple stakeholders. Ocean Coast. Manag., 51, 10, 712 - 726. https://doi.org/10.1016/j.ocecoaman.2008.06.014

Coleman, M., Huh, O.K., 2004. Major deltas of the world: A perspective from space. Coastal Studies Institute, Louisiana State University, Baton Rouge, LA. (www.geol.lsu.edu/WDD/PUBLICATIONS/CandHnasa04/CandHfinal04.htm.)

Corenblit, D., Tabacchi, E., Steiger, J., Gurnell, A.M., 2007. Reciprocal interactions and adjustments between fluvial landforms and vegetation dynamics in river corridors: A review of complementary approaches. Earth Sci. Rev., 84, 1, 56 - 86. https://doi.org/10.1016/j.earscirev.2007.05.004

Doody, J.P., 2004. 'Coastal squeeze': An historical perspective. J. Coast. Conserv., 10, 1-2, 129–138. http://www.jstor.org/stable/25098445

Fletcher, C., Richmond, B., Rooney, J., Barbee, M., Lim, S.C., 2003. Mapping shoreline change using digital orthophotogrammetry on Maui, Hawaii. J. Coast Res., SI 38, 106–124. https://www.jstor.org/stable/25736602

Furukawa, K., Wolanski, E., Mueller, H., 1997. Currents and sediment transport in mangrove forests, Estuarine, Coast. Shelf Sci., **44,** 3, 301. https://doi.org/10.1006/ecss.1996.0120

Gedan, K.B., Kirwan, M.L., Wolanski, E., Barbier, E.B., Silliman, B.R., 2011. The present and future role of coastal wetland vegetation in protecting shorelines: answering recent challenges to the paradigm. Clim. Change, 106, 1, 7–29. https://doi.org/10.1007/s10584-010-0003-7

General statistics office of Vietnam. statistical data., 2015. https://www.gso.gov.vn/Default_en.aspx?tabid=491. (Accessed: 1 April 2015)

Gilman, E., Ellison, J., Coleman, R., 2007. Assessment of mangrove response to projected relative sea-level rise and recent historical reconstruction of shoreline position. Environmental Monitoring and Assessment, 124, 1, 105–130. https://doi.org/10.1007/s10661-006-9212-y

Gilman, E.L., Ellison, J., Jungblut, V., Van Lavieren, H., Wilson, L., Areki, F., Brighouse, G, Bungitak, J, Dus, E, Henry, M, Kilman, M, Matthews, E., 2006. Adapting to Pacific Island mangrove responses to sea level rise and climate change. Clim. Res., 32, 3, 161–176. https://doi.org/10.3354/cr032161

Gratiot, N., Bildstein, A., Anh, T.T., Thoss, H., Denis, H., Michallet, H. and Apel, H., 2017. Sediment flocculation in the Mekong river estuary, Vietnam, an important driver of geomorphological changes. Comptes rendus Geosciences, 349 (6), 260-268.

Gupta, A., 2009. Chapter 3 - geology and landforms of the Mekong basin. In I.C. Campbell (Ed.), The Mekong: Biophysical Environment of an International River Basin (29 – 51). San Diego: Academic Press. https://doi.org/10.1016/B978-0-12-374026-7 .00003-6

Ha, D.T., Ouillon, S. and Vinh, G.V. 2018. Water and suspended sediment budgets in the Lower Mekong from high-frequency measurements (2009-2016). Water, 10(7), 846. https://doi.org/10.3390/w10070846

Hapke, C.J., Reid, D., Richmond, B.M., Ruggiero, P., List, J., 2006. National Assessment of Shoreline Change Part 3: Historical Shoreline Change and Associated Coastal Land Loss Along Sandy Shorelines of the California Coast (Tech. Rep.). U.S. Geological Survey, 1219, 79 pp.

Hashim, A.M., Catherine, S.M.P., 2013. A laboratory study on wave reduction by mangrove forests. APCBEE Procedia, 5, 27 – 32. 4th International Conference on Environmental Science and Development ICESD. https://doi.org/10.1016/j.apcbee.2013.05.006

Heatherington, C., Bishop, M.J., 2012. Spatial variation in the structure of mangrove forests with respect to seawalls. Mar. Freshwater Res., 63, 926–933. https://doi.org/10.1071/MF12119

Himmelstoss, E.A., Henderson, R.E., Kratzmann, M.G., and Farris, A.S., 2018, Digital Shoreline Analysis System (DSAS) version 5.0 user guide: U.S. Geological Survey Open-File Report 2018–1179, 110 p., https://doi.org/10.3133/ofr20181179.

Horstman, E.M., Dohmen-Janssen, C.M., Narra, P.M.F., Van den Berg, N.J.F., Siemerink, M., Hulscher, S.J.M.H., 2014. Wave attenuation in mangroves: a quantitative approach to field observations. Coast. Eng., 94, 47–62. https://doi.org/10.1016/j.coastaleng.2014.08.005

Jhaveri, N., Nguyen, T.D., Nguyen, K.D., 2018. Mangrove collaborative management in Vietnam and Asia. USAID Report, 70 pp.

Kathiresan, K., 2003. How do mangrove forests induce sedimentation? Revista de Biologia Tropical, 51, 355–360.

Kéfi, S., Holmgren, M., Scheffer, M., 2016. When can positive interactions cause alternative stable states in ecosystems? Funct. Ecol., 30, 1, 88-97. https://doi.org/10.1111/1365-2435.12601

Koehnken, L., 2014. Discharge Sediment Monitoring Project (DSMP) 2009 – 2013 Summary & Analysis of Results. Final Report, Mekong River Commission, Lao PDR, 126 pp.

Kumara, M.P., Jayatissa, L.P., Krauss, K.W., Phillips, D.H., Huxham, M., 2010. High mangrove density enhances surface accretion, surface elevation change, and tree survival in coastal areas susceptible to sea-level rise. Oecologia, 164, 2, 545–553. https://doi.org/10.1007/ s00442-010-1705-2

Li, X., Liu, J.P., Saito, Y., Nguyen, V.L., 2017. Recent evolution of the Mekong delta and the impacts of dams. Earth Sci. Rev., 175, 1 – 17. https://doi.org/10.1016/j.earscirev.2017.10.008

Marchesiello, P., Nguyen, N.M., Gratiot, N., Anthony, E.J., Nguyen, T., Almar, R., Kestenare, E., 2019. Erosion of the coastal Mekong delta: assessing natural against man induced processes. Cont. Shelf Res., 181, 72-89. https://doi.org/10.1016/j.csr.2019.05.004

Marois, D.E., Mitsch, W.J., 2015. Coastal protection from tsunamis and cyclones provided by mangrove wetlands – a review. Int. J. Biodiv. Sci., Ecosyst. Serv. Manag., 11, 71–83.

Massel, S., Furukawa, K., Brinkman, R., 1999. Surface wave propagation in mangrove forests. Fluid Dyn. Res., 24, 4, 219 - 249. https://doi.org/10.1016/S0169-5983(98)00024-0

Mazda, Y., Magi, M., Kogo, M., Hong, P.N., 1997. Mangroves as a coastal protection from waves in the Tong king delta, Vietnam. Mangroves Salt Marshes, 1, 2, 127–135. https://doi.org/10.1023/A:1009928003700

McKee, K.L., Cahoon, D.R., Feller, I.C., 2007. Caribbean mangroves adjust to rising sea level through biotic controls on change in soil elevation. Glob. Ecol. Biogeogr., 16, 5, 545-556. https://doi.org/10.1111/j.1466-8238.2007.00317.x

Mekong River Commission, 2010. State of the basin report. 123 pp. Vientiane, Lao PDR. ISBN 978-993-2080-57-1

Minderhoud, P.S.J., Erkens, G., Pham, V.H., Bui, V.T., Erban, L., Kooi, H., Stouthamer, E., 2017. Impacts of 25 years of groundwater extraction on subsidence in the Mekong delta, Vietnam. Environmental Research Letters, 12, 064006.

Mitra, A., 2013. How mangroves resist natural disaster. In A. Mitra (Ed.), Sensitivity of mangrove ecosystem to changing climate. 107–129. Springer India. https://books.google.fr/books?id=sXc8AAAAQBAJ

Phan, L.K., van Thiel de Vries, J.S., Stive, M.J., 2015. Coastal mangrove squeeze in the Mekong delta. J. Coast. Res., 233-243. https://doi.org/10.2112/JCOASTRES-D-14-00049.1

Phan, N.H., Hoang, T.S., 1993. Mangroves of Vietnam. 173 pp. IUCN, Bangkok. ISBN 283170166X

Piman, T., Shrestha, M., 2017. Case Study on Sediment in the Mekong River Basin: Current State and Future Trends. UNESCO and Stockholm Environment Institute (SEI), 48 pp.

Pontee, N., 2013. Defining coastal squeeze: A discussion. Ocean Coast. Manag., 84, 204 – 207. https://doi.org/10.1016/j.ocecoaman.2013.07.010

Proisy, C., Gratiot, N., Anthony, E.J., Gardel, A., Fromard, F., Heuret, P. 2009. Mud bank colonization by opportunistic mangroves: a case study from French Guiana using lidar data. Continental Shelf Research, 29, 632–641.

Quartel, S., Kroon, A., Augustinus, P., Santen, P.V., Tri, N., 2007. Wave attenuation in coastal mangroves in the red river delta, Vietnam. Journal of Asian Earth Sciences, 29 (4), 576 – 584. https://doi.org/10.1016/j.jseaes.2006.05.008

Rooney, J., Fletcher, C., Barbee, M., Eversole, D., Lim, S.-c., Richmond, B., Gibbs, A., 2003. Dynamics of sandy shorelines in Maui, Hawaii - Soest Hawaii: Consequences and causes. In Coastal sediments (1–14). Florida.

Ruggiero, P., List, J.H., 2009. Improving accuracy and statistical reliability of shoreline position and change rate estimates. Journal of Coastal Research, 25, 1069-1081.

Torio, D.D., Chmura, G.L., 2013. Assessing coastal squeeze of tidal wetlands. Journal of Coastal Research, 29, 1049–1061.

Van Wesenbeeck, B., Balke, T., van Eijk, P., Tonneijck, F., Siry, H., Rudianto, M., Winterwerp, J., 2015. Aquaculture induced erosion of tropical coastlines throws coastal communities back into poverty. Ocean and Coastal Management, 116, 466 - 469. https://doi.org/10.1016/j.ocecoaman.2015.09.004

Veettil, B.K., Ward, R.D., Quangf, N.X., Trang, N.T.T., Giang, T.H., 2019. Mangroves of Vietnam: Historical development, current state of research and future threats. Estuarine, Coastal and Shelf Science, 218, 212-236. https://doi.org/10.1016/j.ecss.2018.12.021

Vidthayanon C. 2008. Field guide to fishes of the Mekong Delta. Mekong River Commission, Vientiane, Lao PDR. 288 pp.

Winterwerp, J.C., Erftemeijer, P.L.A., Suryadiputra, N., Van Eijk, P., Zhang, L., 2013. Defining eco-morphodynamic requirements for rehabilitating eroding mangrove-mud coasts. Wetlands, 33, 515–526.

Woodroffe, C., Rogers, K., McKee, K., Lovelock, C., Mendelssohn, I., and Saintilan, N., 2016. Mangrove sedimentation and response to relative sea-level rise. Annual Review of Marine Science, 8 (1), 243-266. https://doi.org/10.1146/annurev-marine-122414-034025

World Wide Fund for Nature, 2012. Ecological footprint and investment in natural capital in Asia and the Pacific. ©Asian Development Bank and World-Wide Fund for Nature. CC BY-NC IGO 3.0. 104 pp. http://hdl.handle.net/11540/895

FIGURE CAPTIONS

Figure 1. Map of the Mekong River delta showing shoreline change between 2003 and 2012 (from Anthony et al., 2015) in the three shoreline sectors: the sand-dominated delta distributary mouths, and the muddy East and West Coasts. Small rectangle on the East coast shoreline shows location of shoreline examples depicted in Fig. 2.

Figure 2. Examples of shorelines and positioning of the mangrove edge for digitization (see location in Fig. 1).

Figure 3. Graph showing the variation of Mekong delta shoreline change rates from 2003 to 2012 with mangrove width in 2012 (each dot corresponds to a transect), and discrimination of the three shoreline sectors (red dots for delta distributary mouths, black dots for East Coast, blue dots for West Coast). The six histograms show the frequency distribution for each sector with regards to mangrove width (left), and shoreline change (right).

Figure 4. Graphs showing the number (top) and the percentage (bottom) of transects in erosion among all transects in the different classes of 0.1 km mangrove-width range.

Figure 5. Locations of the 10% of shoreline sectors exhibiting a significant correlation between width of fringing vegetation and erosion/accretion. Of this, mangroves represent less than 5%.

Supplementary material

Comparison of the relationship between mangrove width and shoreline change based on the 2003 (a) and 2012 (b) satellite images.

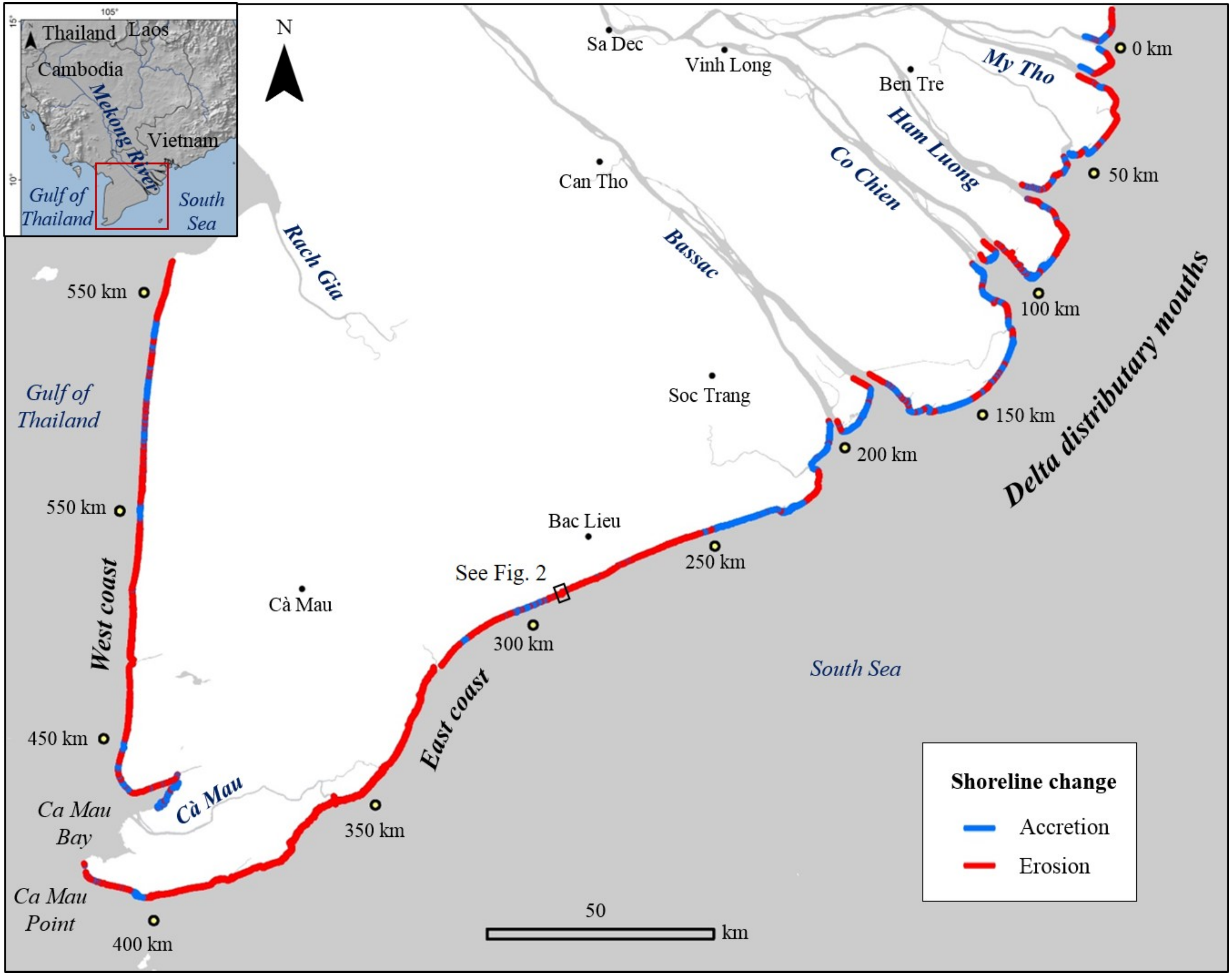

105°
15°
10°
Thailand
Laos
Cambodia
Mekong River
Vietnam
Gulf of Thailand
South Sea
N
Sa Dec
Vinh Long
Ben Tre
My Tho
0 km
Ham Luong
Co Chien
50 km
Can Tho
Bassac
Rach Gia
100 km
550 km
Gulf of Thailand
Soc Trang
150 km
200 km
Delta distributary mouths
550 km
Bac Lieu
250 km
See Fig. 2
Cà Mau
300 km
West coast
South Sea
East coast
450 km
Cà Mau
Ca Mau Bay
350 km
Shoreline change
Accretion
Erosion
Ca Mau Point
400 km
50
km

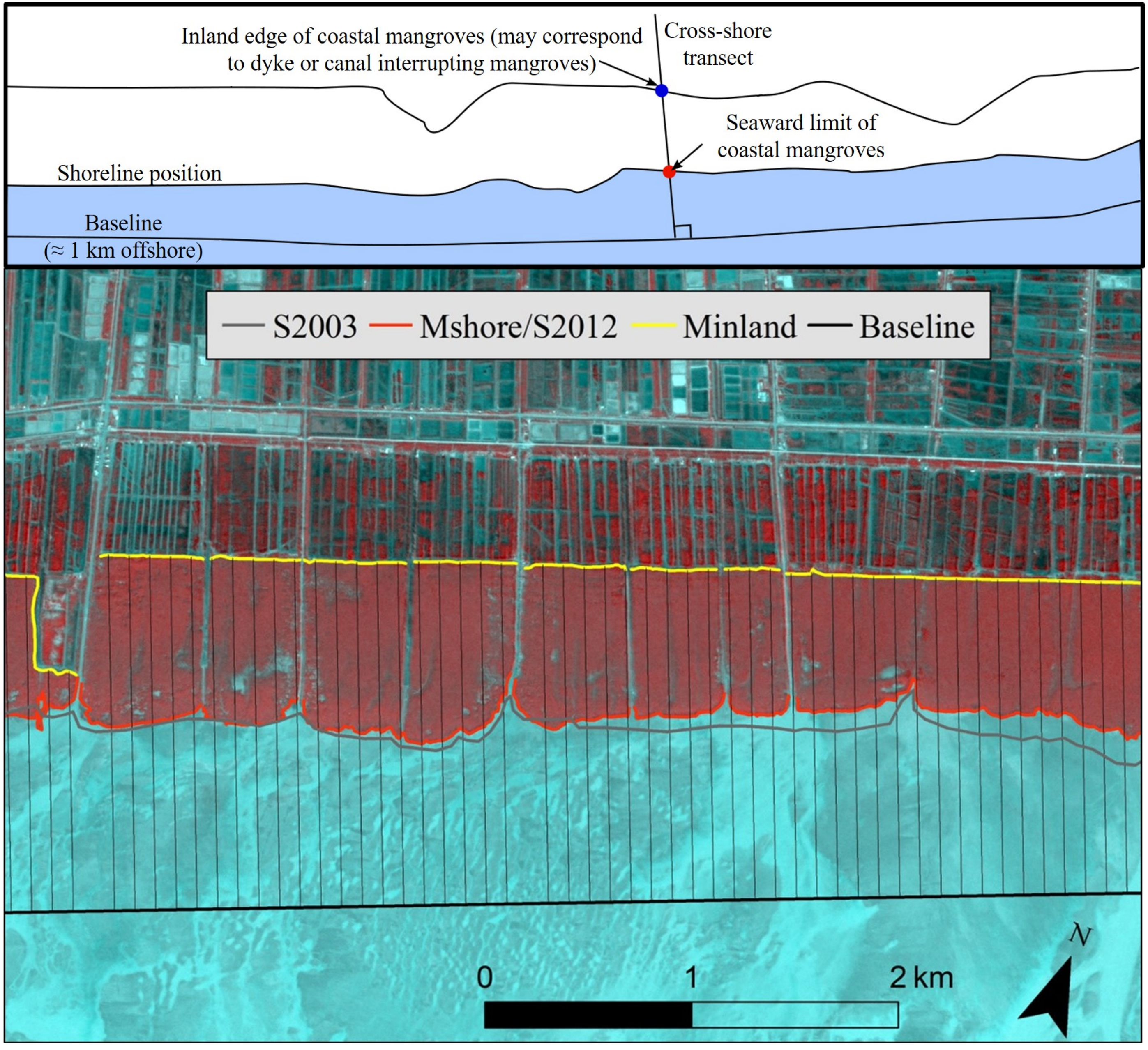

Inland edge of coastal mangroves (may correspond to dyke or canal interrupting mangroves)
Cross-shore transect
Seaward limit of coastal mangroves
Shoreline position
Baseline (≈ 1 km offshore)
S2003
Mshore/S2012
Minland
Baseline
0
1
2 km
N

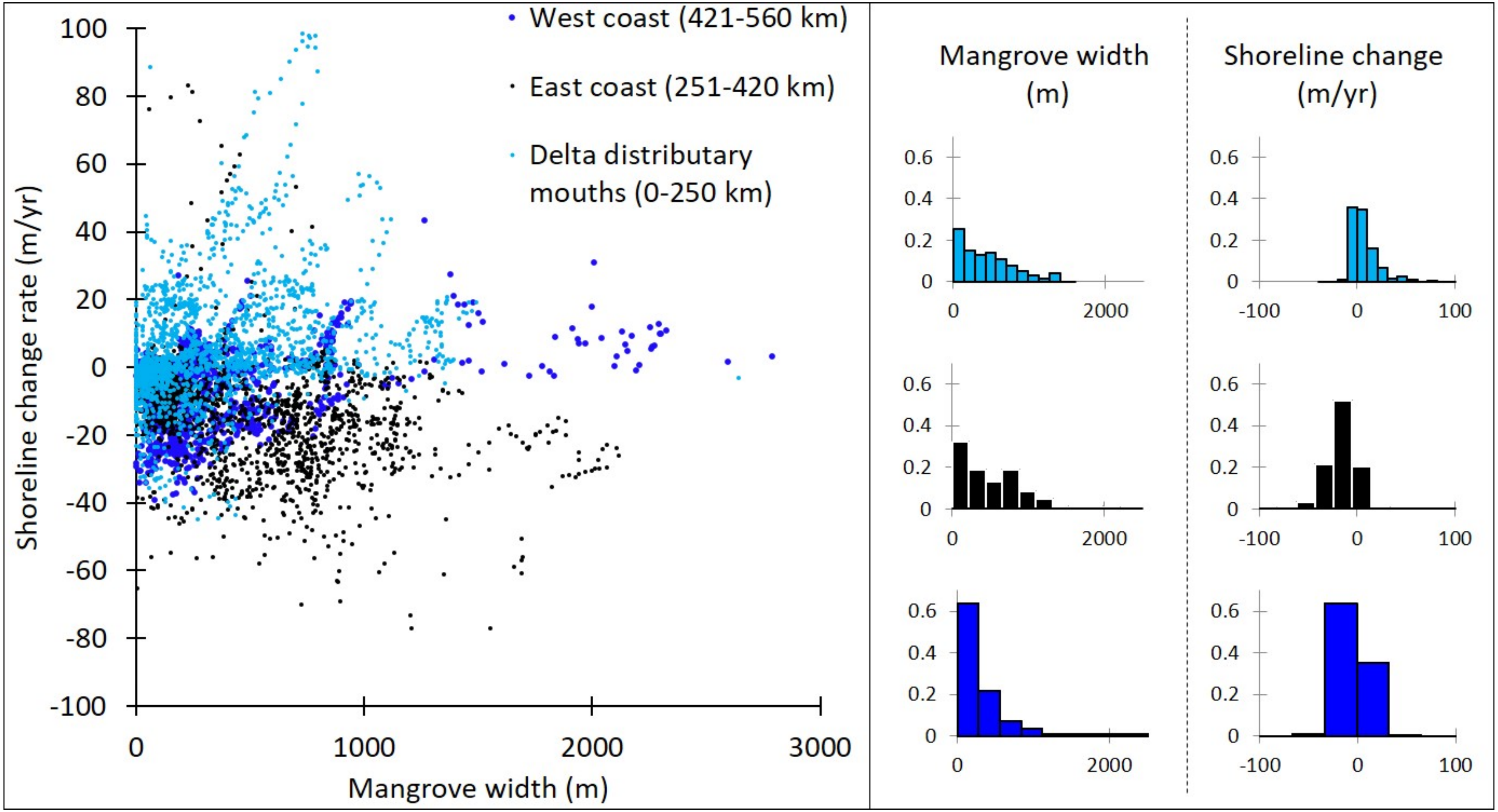
West coast (421-560 km)
East coast (251-420 km)
Delta distributary mouths (0-250 km)
Shoreline change rate (m/yr)
Mangrove width (m)
100
80
60
40
20
0
-20
-40
-60
-80
-100
0
1000
2000
3000
Mangrove width (m)
Shoreline change (m/yr)
0.6
0.4
0.2
0
0
2000
-100
0
100

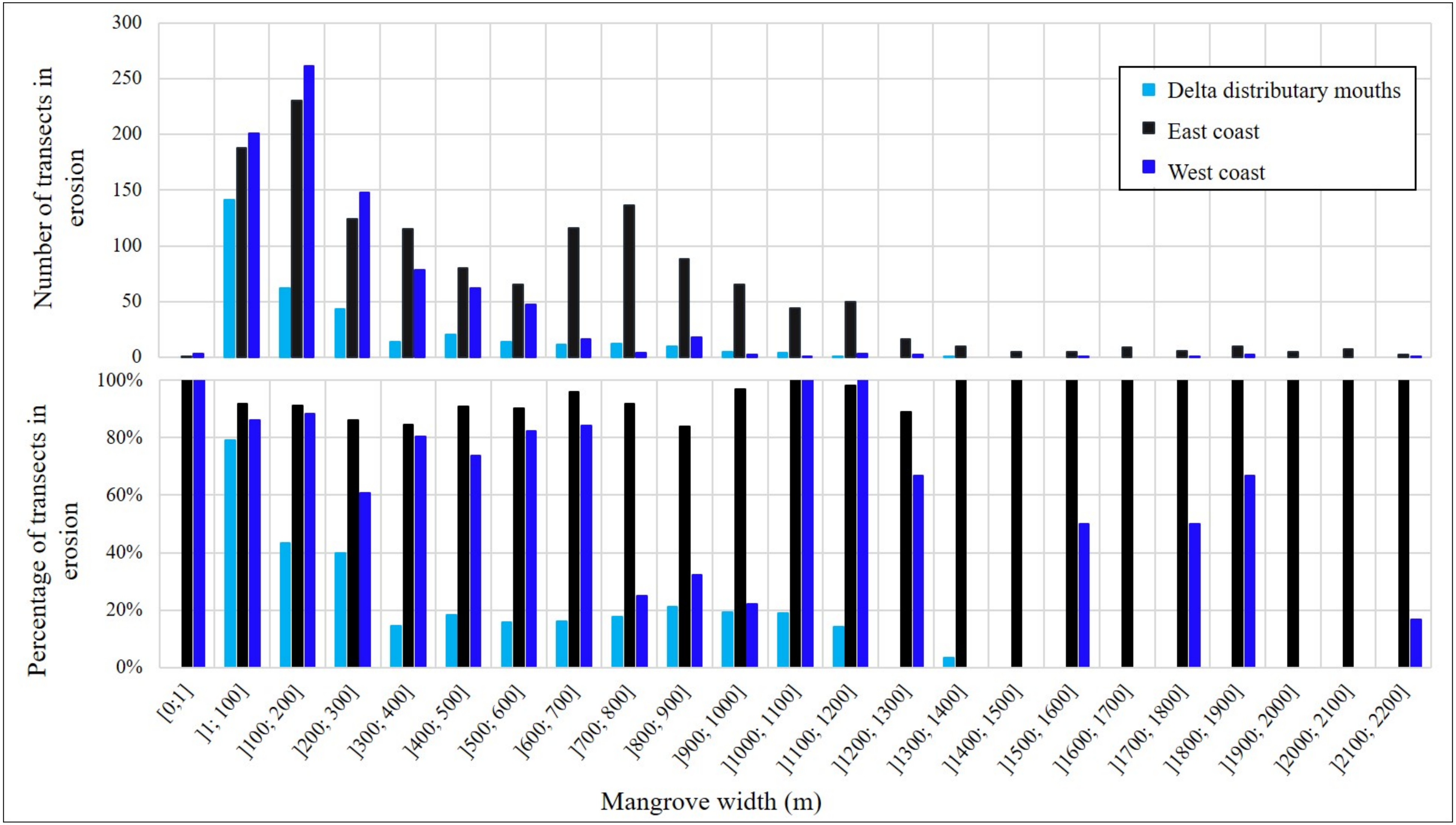

Number of transects in erosion
Percentage of transects in erosion
Delta distributary mouths
East coast
West coast
Mangrove width (m)
300
250
200
150
100
50
0
100%
80%
60%
40%
20%
0%
[0;1]
]1; 100]
]100; 200]
]200; 300]
]300; 400]
]400; 500]
]500; 600]
]600; 700]
]700; 800]
]800; 900]
]900; 1000]
]1000; 1100]
]1100; 1200]
]1200; 1300]
]1300; 1400]
]1400; 1500]
]1500; 1600]
]1600; 1700]
]1700; 1800]
]1800; 1900]
]1900; 2000]
]2000; 2100]
]2100; 2200]

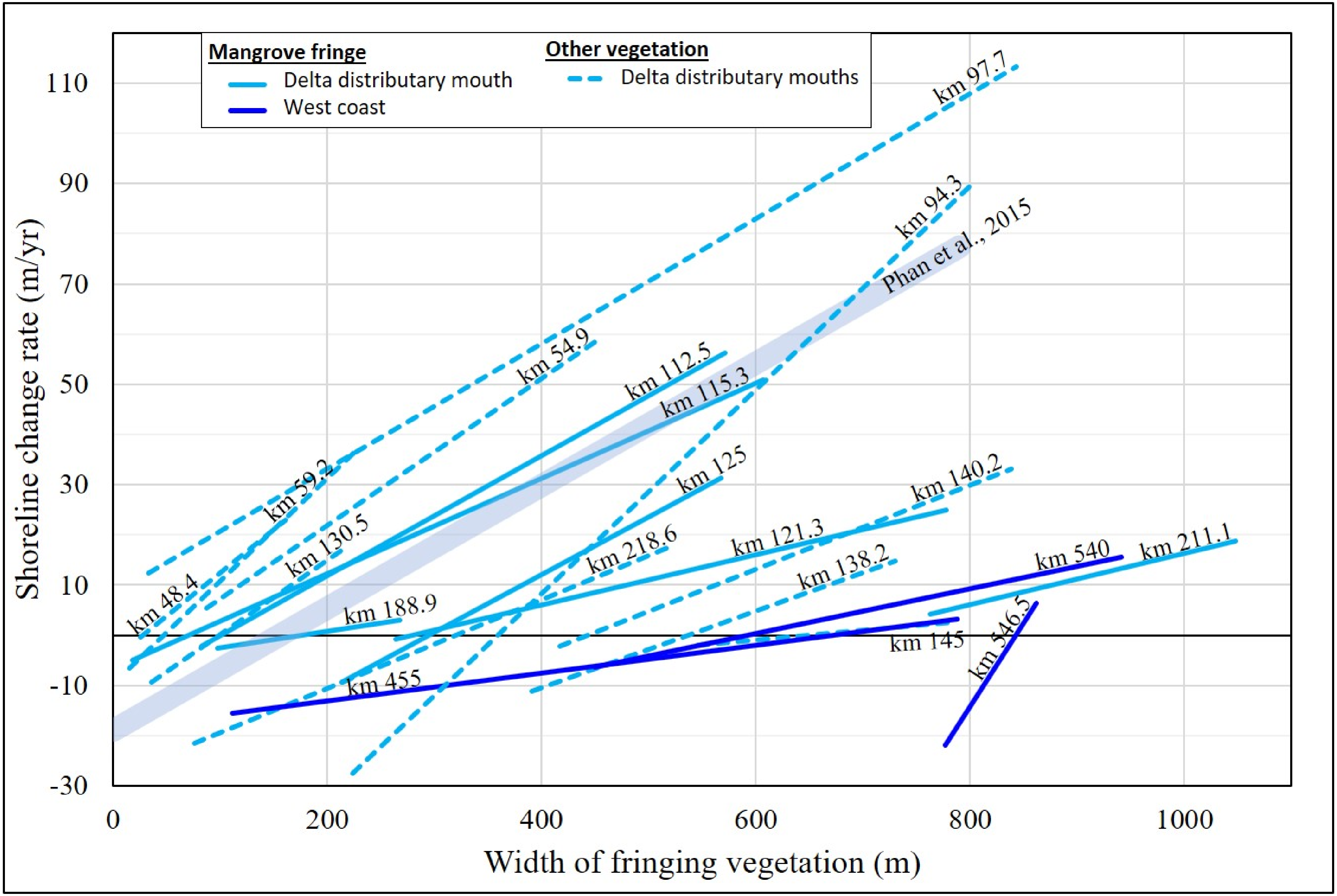

Mangrove fringe
Delta distributary mouth
West coast
Other vegetation
Delta distributary mouths
km 97.7
km 94.3
Phan et al., 2015
km 54.9
km 112.5
km 115.3
km 59.2
km 130.5
km 125
km 140.2
km 218.6
km 121.3
km 48.4
km 188.9
km 138.2
km 540
km 211.1
km 546.5
km 145
km 455
Shoreline change rate (m/yr)
Width of fringing vegetation (m)
110
90
70
50
30
10
-10
-30
0
200
400
600
800
1000

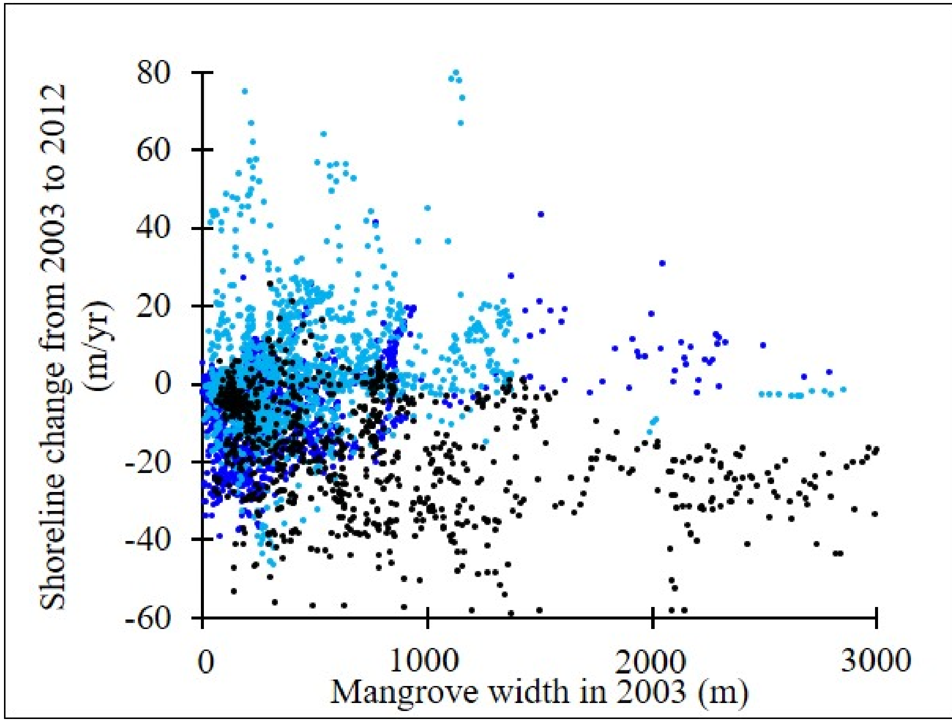
Shoreline change from 2003 to 2012 (m/yr)
Mangrove width in 2003 (m)
80
60
40
20
0
-20
-40
-60
0
1000
2000
3000
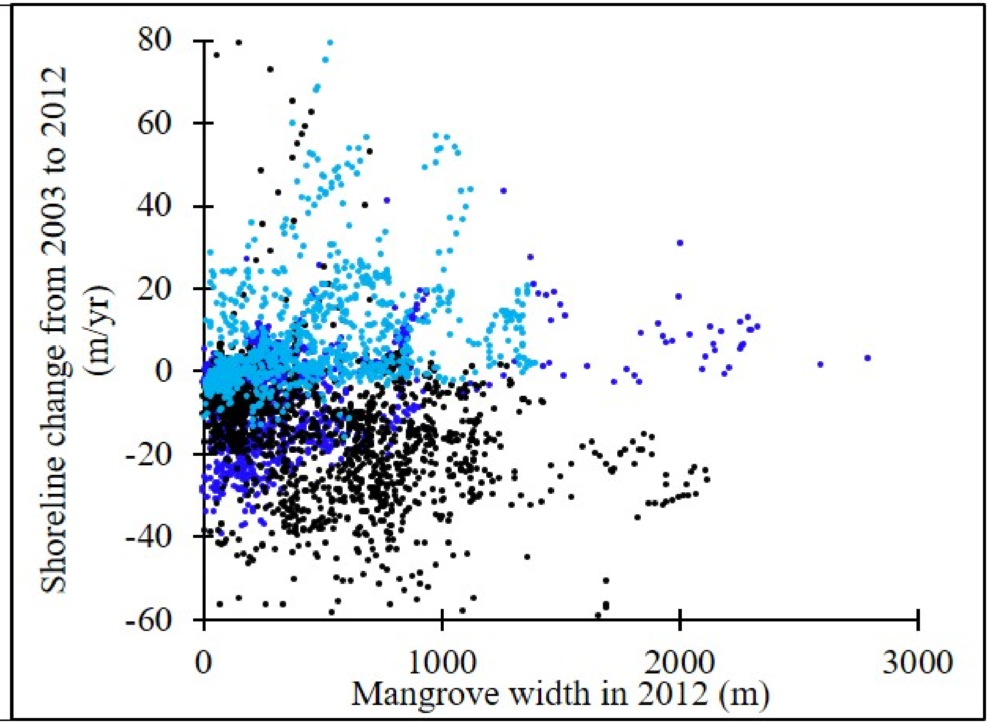
Shoreline change from 2003 to 2012 (m/yr)
Mangrove width in 2012 (m)
80
60
40
20
0
-20
-40
-60
0
1000
2000
3000